Ligand Specificity of Constitutive Androstane Receptor as Probed by Induced-Fit Docking and Mutagenesis

Susanna Repo,[†] Johanna Jyrkkärinne,[‡] Juha T. Pulkkinen,[§] Reino Laatikainen,[§] Paavo Honkakoski,*[,‡] and Mark S. Johnson*[,†]

Structural Bioinformatics Laboratory, Department of Biochemistry and Pharmacy, Åbo Akademi University, Tykistökatu 6, FI-20520 Turku, Finland, Department of Pharmaceutics, University of Kuopio, P.O. Box 1627, FI-70211 Kuopio, Finland, and Laboratory of Chemistry, Department of Biosciences, University of Kuopio, P.O. Box 1627, FI-70211 Kuopio, Finland

Received March 25, 2008

Constitutive androstane receptor (CAR, NR1I3) belongs to the nuclear receptor family of transcription factors and acts as a chemical sensor of drugs and endogenous compounds. The ligand-binding preferences of CAR are diverse, and more importantly, there are significant species differences in ligand specificity. Here, we show that while certain residues are critical for the basal activity of mouse CAR (mCAR) and/or affect the binding of all tested ligands, mutation of some ligand-binding pocket (LBP) residues (e.g., F171 and Y336) paradoxically decreased the activity of a specific ligand while increasing that of others. Comparisons to previously reported human CAR (hCAR) residues indicated that the function of key CAR residues (e.g., N175, L253) is dramatically different between species. The docking results provide some mechanistic rationale for the ability of 17α-ethinyl-3,17β-estradiol (EE2) to both activate mCAR and repress hCAR.

1. Introduction

Nuclear receptors (NRs[a]) comprise a superfamily of 48 transcription factors that control cellular development, homeostasis, and metabolism by responding to small molecule ligands.[1−3] NRs are structurally modular, and with few exceptions they consist of an N-terminal region housing the transcriptional activation function 1 (AF-1), a well-conserved DNA-binding domain, and the C-terminal ligand binding domain (LBD).[4] The solved crystal structures of NR LBDs have revealed that ligand binding induces conformational changes in the LBD structure, of which the most important is the ligand-induced movement of the C-terminal helix H12. In the active conformation, helix H12 is packed firmly on top of the ligand binding pocket (LBP) and residues from helix H12 contribute to the formation of activation function 2 (AF-2), which acts as the interaction surface for NR coactivators.[5] Upon binding to the LBD, NR coactivators are able to mediate the activation signal to NR target gene promoters via local histone acetylation, chromatin decondensation, recruitment of mediating factors, and ultimately, activation of the preinitiation complex.[6,7] Antagonist binding prevents the H12 helix from adopting the active conformation, which disrupts AF-2, and subsequently, NR corepressors may bind to the LBD.[5] The presence of corepressors leads to histone deacetylation, chromatin condensation, and finally, gene repression.[7,8]

The mouse constitutive androstane receptor (mCAR, NR1I3) acts as a chemical sensor that regulates genes involved in the oxidative and conjugative metabolism of drugs and endogenous compounds and their subsequent elimination from the cells via various efflux and transport proteins (for reviews, see refs 9−11). Distinct from most other NRs, mCAR shows remarkable basal activity[12] that is enhanced upon heterodimerization with the retinoid X receptor (RXR).[13] Heterodimerization induces allosteric stabilization on the mCAR LBD, which in turn triggers coactivator interaction and transcriptional activity. The basal activity of mCAR can be suppressed by an inverse agonist, 5α-androst-16-en-3α-ol (androstenol),[14] while several cytochrome P450 (CYP) enzyme inducers act as mCAR agonists that can reactivate mCAR after its suppression by androstenol.[9,15−17]

Crystal structures of mCAR in complex with both the super-agonist 1,4-bis[2-(3,5-dichloropyridyloxy)]benzene (TCPOBOP) and the inverse agonist androstenol have been solved.[18,19] These structures suggest that the high basal activity of mCAR is based on a compact LBD structure with an extended helix H2 that stabilizes the overall fold. In contrast, the H12 helix of mCAR is exceptionally short, which enables the formation of stabilizing salt bridges between H12 and helices H4 and H10, although dissenting views about the role of the length of helix H12 have been presented.[20,21] In addition, there is a short linker helix located between helices H10 and H12, which restricts the movement of H12 and stabilizes the active conformation (for a recent review, see ref 22). The short length of the linker helix has been speculated to be crucial for the constitutive activity of mCAR but not for the agonist-induced activity.[13] However, the exact role of this linker helix is unclear because the ligand-free structure of mCAR has not yet been reported and similar helices are present in other ligand-bound NR LBDs.[21,22]

Previously, we reported a 3D-QSAR analysis of mCAR inhibition by over 40 steroids.[23] These analyses indicated that only a well-defined and predictable set of steroids could inhibit mCAR while a large group of diverse chemicals including estrogens were agonists of mCAR.[24] One of the steroids, 17α-ethinyl-3,17β-estradiol (EE2) which was shown to activate mCAR, acts as an inhibitor on human CAR,[25] indicating that there are species differences in ligand recognition. This has been

* To whom correspondence should be addressed. For P.H.: phone, +358-40 355 2490; fax, +358-17-162 456; e-mail, paavo.honkakosi@uku.fi. For M.S.J.: phone, +358-2-2154014; fax, +358-2-2153280; e-mail, johnson4@abo.fi.

† Åbo Akademi University.

‡ Department of Pharmaceutics, University of Kuopio.

§ Department of Biosciences, University of Kuopio.

[a] Abbreviations: AF-1 and AF-2, activation function-1 and -2; βGAL, β-galactosidase; DMSO, dimethyl sulfoxide; EE2, 17α-ethinyl-3,17β-estradiol; hCAR, human constitutive androstane receptor; IFD, induced-fit docking; LBD, ligand binding domain; LBP, ligand binding pocket; M1H, mammalian one-hybrid; mCAR, mouse constitutive androstane receptor; NCoR, nuclear receptor corepressor; NLS, nuclear localization signal; NR, nuclear receptor; SRC-1, steroid receptor coactivator-1; SP, standard precision; TCPOBOP, 1,4-bis[2-(3,5-dichloropyridyloxy)]benzene; XP, extra precision; Y2H, yeast two-hybrid.

10.1021/jm800337r CCC: $40.75 © 2008 American Chemical Society
Published on Web 10/31/2008

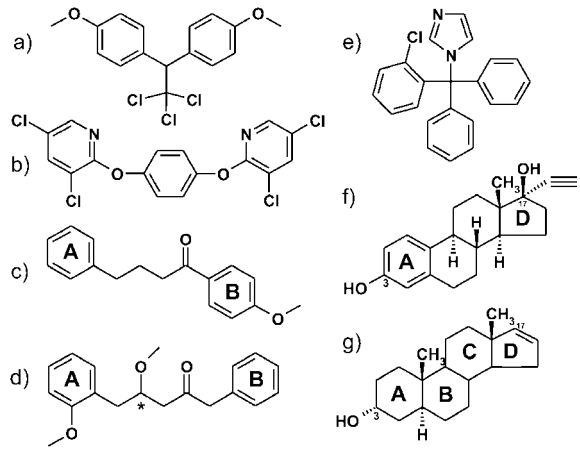

Figure 1. Structures of the ligand molecules investigated in this study: (a) methoxychlor, (b) TCPOBOP), (c) compound **1**, (d) compound **2**, (e) clotrimazole, (f) EE2, and (g) androstenol.

further demonstrated with other CAR ligands, too[17,24,25] (reviewed in ref 26).

Despite knowledge of the solved crystal structures of the mCAR LBD in complex with ligands, the basis of the promiscuous nature of mCAR ligand binding has not yet been elucidated. In order to gain more insight on how mCAR activity is modulated by ligands, we analyzed TCPOBOP, androstenol, and known mCAR activating compounds,[24] clotrimazole (1-[(2-chlorophenyl)diphenylmethyl]imidazole), methoxychlor (1,1,1-trichloro-2,2-bis(4-methoxyphenyl)ethane), and EE2, for their effects (see Figure 1 for the molecular structures of the investigated ligands). In addition, we included two very flexible compounds,[27] 1-(4-methoxyphenyl)-4-phenylbutan-1-one, **1**, and 4-methoxy-5-(2-methoxyphenyl)-1-phenylpentan-2-one, **2**, from a focused set of estrogen receptor ligands[28] that displayed significant mCAR activation in pilot studies (data not shown). Site-directed mutagenesis revealed that while certain residues are critical for the basal activity of mCAR and/or affect the binding of all ligands, mutation of some residues paradoxically decreased the activity of a specific ligand while increasing that of others. The mutation of mCAR residues to the human counterparts indicated that the ligand specificity of mCAR cannot be changed solely by a single residue mutation similarly to what has been observed with hCAR.[25] The possible binding modes of the analyzed ligands were elucidated with molecular docking studies using the induced-fit effect to introduce flexibility into the receptor structure during docking. The induced-fit protocol proved to be a more suitable approach for docking ligands to the mCAR LBP than the rigid-body docking procedure, and the results presented here emphasize the remarkable flexibility of the mCAR LBP in ligand recognition.

2. Results

Modulation of the Basal Activity of mCAR. Altogether, 10 amino acids in the LBP of mCAR were mutated in this study (see Figure 2 for the location of the residues within the LBP). The mutations were selected either based on interspecies differences between human and mouse CAR[23,25] (S251L, I252L, L253F, and T350M) or based on the analysis of the crystal structures of mCAR[18,19] (F171A, F171L, N175A, L212A, H213A, Y336A, T350A, and L353A).

The basal activities of the 12 mutants were measured with mammalian one-hybrid (M1H) trans-activation assays, and the results are presented in Supporting Information Figure S1. In

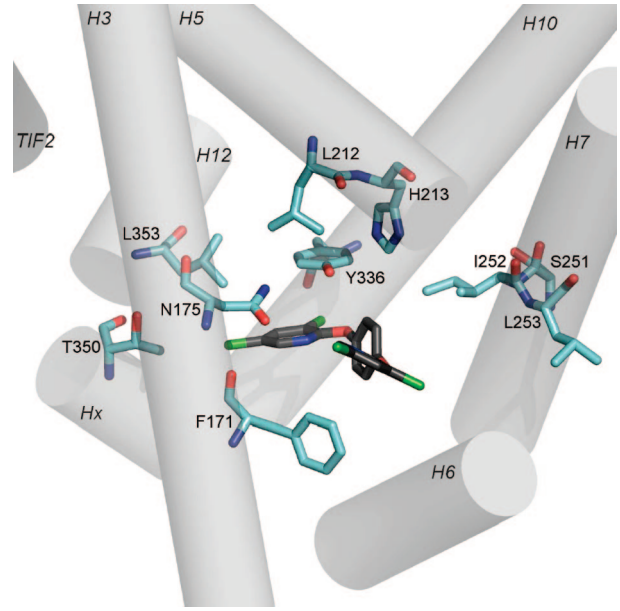

Figure 2. Crystal structure of mCAR bound with TCPOBOP and in complex with the coactivator peptide TIF2.[19] The helices are labeled and shown as cylinders, and the bound TCPOBOP is presented as a stick figure with black carbon atoms and green chloride atoms. The amino acids that were mutated in this study are labeled and shown as stick figures with carbon atoms in cyan, nitrogens atoms in blue, and oxygens atoms in red.

addition, the effects of seven ligand molecules (TCPOBOP, clotrimazole, methoxychlor, **1**, **2**, EE2, and androstenol) on the basal activity of mCAR were investigated. The high basal activity of wild-type mCAR was further increased by TCPOBOP and **2** (2.0-fold), modestly by other agonists (about 40%), and decreased by over 60% with the inverse agonist androstenol. The mutation L353A in helix H12 decreased the basal activity of mCAR to 13%, while F171A induced a smaller decrease to 30%. The two T350 mutations in the linker helix, T350A and T350M, increased the basal activity of mCAR to 150% and 133%, respectively. In most cases with reduced basal activity (F171A, L212A, H213A, Y336A), the basal activity of the corresponding hCAR mutations also decreased.[25] The only exceptions were N175A and T350 mutations that exhibited a decrease with the human receptor only.

The M1H assay measures the net effect of ligand-induced recruitment of *all* coactivators and corepressors present and able to interact with the mCAR LBD in the transfected cells. In contrast, the yeast two-hybrid (Y2H) system we employed is assaying individual, ligand-dependent interactions between the mCAR LBD and the prototype coactivator SRC-1 or the corepressor NCoR. Thus, by use of Y2H assays, it is possible to gain some mechanistic explanations for the observed activity changes. However, it is possible that some effects on receptor activity may result from the ligand- or mutation-specific recruitment of cellular coregulators other than SRC-1 or NCoR, as already shown for hCAR mutations[25] or for ligands of the estrogen receptor.[29] The results from the Y2H assays with SRC-1 and NCoR are presented in Supporting Information Figure S2a and Figure S2b, respectively. Notably, all agonists could further enhance by 2.5- to 3.4-fold the high basal interaction between wild-type mCAR and the SRC-1, while the inverse agonist androstenol was without effect. The weak basal interaction with NCoR was dramatically increased by EE2 and

Table 1. Summary of the Mammalian Trans-Activation Data of mCAR Mutants and the Tested Ligands

	F171A	F171L	N175A	L212A	H213A	S251L	I252L	L253F	Y336A	T350A	T350M	L353A
TCPOBOP	–[a]	–	▼[b]	▲[c]	▲	▼	▲	–	–[d]	▼	▼	▼
clotrimazole	▲	▼	▼	▲	–	▼	▲	▼	▼	▼	▲	▼
methoxychlor	▲	▼	▼	▲	–	▼	▼	–	▲	▼	–	▼
1	▲	▲	▼	▲	▼	▼	▼	▼	▼	▼	▼	▼
2	▲	–	▼	▲	▼	▼	▼	▼	–	▼	▼	▼
EE2	▲	–	▼	▲	▼	▼	▼	▲	▼	▼	▼	▼
androstenol	▼	▼	▼	▼	▼	▲	▼	▼	▼	▲	–	▼

[a] No change in ligand response. Gray highlight indicates in silico observed contacts between the corresponding ligand and amino acid. [b] Down-pointing triangles indicate decrease in ligand response (in the case of androstenol, decrease in inhibition or even activation): (small ▼) <50%; (medium ▼) 50−100%; (large ▼) activity < DMSO. [c] Up-pointing triangles indicate increase in ligand response (in the case of androstenol, increase in inhibition): (small ▲) <50%; (medium ▲) 50−100%; (large ▲) >100%. [d] Red color indicates that the change in the M1H activation profile cannot be explained by SRC-1 and NCoR data from the Y2H assays.

Table 2. Summary of the Main Effects of the Mutations on Ligand-Induced Coregulator Interactions with mCAR As Measured by the Yeast Two-Hybrid Assay

		F171A	F171L	N175A	L212A	H213A	S251L	I252L	L253F	Y336A	T350A	T350M	L353A
TCPOBOP	SRC-1	[a]		▼[b]				▲[c]		▼	▼*[d]	▼*	▼
	NCoR												
clotrimazole	SRC-1			▲	▲		▼		▼	▼	▼*		
	NCoR		▲[c]	▼	▼	▲	▼	▲*	▼	▼*	▼	▼	▼
methoxychlor	SRC-1		▲	▼*	▲			▲		▼			
	NCoR	▲		▼	▼	▼*	▼	▲*		▼*	▼	▼	▼
1	SRC-1			▲*				▲*		▼			
	NCoR	▲*	▲	▼		▲	▼	▲		▼*	▼	▼	▲
2	SRC-1		▲	▲	▲			▲		▲		▲*	
	NCoR		▼*	▼	▼		▼	▲*	▼*	▼	▼*	▼	▼*
EE2	SRC-1			▲	▲		▼*						▼
	NCoR			▼	▼	▼	▼	▲	▼	▼*	▼	▼	
androstenol	SRC-1			▲									
	NCoR	▼	▼*	▼	▼	▼	▼	▲	▼	▼	▼	▼	▼

[a] Empty cell: no change or change of <50% in ligand-induced coregulator interaction. [b] Small ▼: decrease of ≥50%. [c] Small ▲: increase of ≥50−150%. [d] ∗: The value of the standard deviation overlaps with the cutoff of the neighboring class. Therefore, the observed change is a trend only and may not be statistically significant. [e] Large ▲: increase of >150%.

androstenol (27- and 49-fold) and significantly by the modest agonists (4- to 10-fold), while the superagonist TCPOBOP had no effect.

The basal interactions between SRC-1 and mCAR were severely reduced (by over 90%) or completely eliminated by the mutation L353A in helix H12 and the mutation H213A in helix H5, respectively. Most of the other mutations decreased the basal interaction of mCAR with SRC-1 by 24−80%, while it was not affected by S251L and T350A and was even slightly enhanced by T350M. The weak basal interaction of the mCAR LBD with NCoR was in general unaffected by any of the mutations except L212A, which resulted in a 6-fold increase in reporter activity. Smaller increases (less than 3-fold) were also seen with the mutations S251L, T350A, T350M, and L353A.

Modulation of the Ligand-Dependent Function of mCAR. The effect of the 12 mutations on the function of each of the 7 ligands was investigated next. The results (for each mutant, compared to the solvent vehicle DMSO) from the M1H assay are presented in Supporting Information Figure S1 and summarized in Table 1. In the Y2H assay with SRC-1, we compared the magnitude of agonist-induced interactions to that obtained with the ligand solvent DMSO (referred to as "minus"-fold, −fold, activation), while for NCoR assay, the reference was the mCAR activity obtained with androstenol. The results of the Y2H-assays are presented in Supporting Information Figure S2 and summarized in Table 2, where the change induced by an mCAR mutation is calculated as the percentage of the −fold activation compared to the wild-type mCAR.

In the M1H assays, the mutation L353A in helix H12 completely abolished the modulating effects of all agonists and androstenol. In addition, the mutations N175A, S251L, and T350A decreased the activity of all agonists but to a more modest degree than L353A (Table 1), while N175A also decreased the androstenol-elicited inhibition. L212A induced a moderate increase in the activation elicited by all tested agonists.

Concerning the individual ligands, the extent of TCPOBOP activation in the M1H assay was decreased by more than 50% by the mutation T350M (Figure 3a) and only modestly by N175A, S251L, and T350A. A slight increase in TCPOBOP activation was observed with I252L. The TCPOBOP-elicited increase in SRC-1 interaction was abolished with the mutant Y336A, an observation that is somewhat surprising because this mutant was still activated by TCPOBOP in the M1H assay (indicated with red color in Table 1). In addition, the mutants N175A, T350A, and T350M strongly reduced the interaction with SRC-1, and increases were observed only with the mutant I252L. It is notable that TCPOBOP could not promote recruitment of the corepressor NCoR with any of the mutants.

The androstenol-mediated inhibition of mCAR was strongly attenuated by L212A and Y336A and completely eliminated by the point mutations F171A, N175A, and H213A (Figure 3b); in fact, androstenol even activated the F171A mutant by 54%. In the Y2H assays, androstenol did not influence the interaction between SRC-1 and the mCAR or its mutants to any great degree. The only exceptions were the robust 8.7-fold increase observed with the mutant N175A and a 40% increase with F171A. In contrast, there was dramatic attenuation (>90%) in NCoR recruitment by androstenol with the mutants F171A, N175A, H213A, and Y336A, while all of the other mutations, except for I252L, decreased the NCoR recruitment moderately. An increase (>200%) in the NCoR recruitment by androstenol was observed with I252L; however, the inhibition by androstenol in M1H assay was slightly decreased by the same mutation.

The available crystal structures of mCAR in complex with TCPOBOP (PDB code 1XLS[19]) and androstenol (PDB code 1XNX[18]) provided a firm basis to evaluate the structural reasons for the observed changes in TCPOBOP- and androstenol-elicited function of the mutated proteins (see Discussion for details). The binding modes of the other five agonists (clotrimazole, methoxychlor, **1**, **2**, and EE2) to mCAR were investigated with ligand docking studies using the induced-fit docking protocol (IFD) and the crystal structure of mCAR in complex with TCPOBOP.[19] More information about the docking procedures are available in the Materials and Methods and in the Supporting Information.

Hereafter, the experimental and docking results for clotrimazole, methoxychlor, **1**, **2**, and EE2 ligands are presented in detail. From the docking studies, the suggested ligand binding modes (most representative poses) for each ligand were manually chosen from clusters of similar poses. Unless otherwise stated, all of the interactions described between the ligand molecules and the receptor are formed by side chain atoms of an amino acid.

Clotrimazole. The modest activation by clotrimazole (1.4-fold) was eliminated by the mutations F171L, N175A, L253F, and Y336A, while it was increased to 2.0- and 3.6-fold by T350M and F171A, respectively. The extent of activation in clotrimazole-induced SRC-1 interaction was markedly reduced (>50%) with the mutants S251L, L253F, Y336A, and T350A, while the mutations N175A and L212A produced an increase of 77% and 73%, respectively. Interestingly, the extent of clotrimazole-induced interaction with NCoR was significantly increased by the mutations F171L and H213A. The clotrimazole-elicited activation in M1H assay did not show any change by H213A mutation. In addition, a moderate increase in M1H assay was observed by I252L, although the same mutation modestly increased the clotrimazole-induced NCoR interaction in the Y2H assay.

In the docking studies, we observed very little variation among the obtained poses for clotrimazole; thus, it seems that in the binding pocket of mCAR there is only one possible location where the bulky clotrimazole molecule could be accommodated. In all of the 55 docking poses, the polar imidazole ring of clotrimazole is positioned within the polar environment formed by N175, H213, and Y336 (see Figure 3c for the binding mode of clotrimazole that appeared to be the most compatible with the binding site). In a great majority of the poses, the chloride atom of clotrimazole is located between the phenyl ring of F227 and the Cβ atom of Y234 and A239; this is the same location where one of the chloride atoms of TCPOBOP is situated in its complex with mCAR in the crystal structure.[19] According to our docking results, there seems to be good aromatic interactions between the three phenyl rings of clotrimazole and F171, F227, Y234, and F244, in addition to hydrophobic interactions with I174, L216, A239, L249, I252, and L253.

Methoxychlor. The activation by methoxychlor (1.4-fold) was absent with the mutations N175A, I252L, and T350A, while a slight increase by Y336A was observed. The −fold extent of methoxychlor-induced interaction with SRC-1 was increased by F171L, L212A, and I252L, while a decrease by N175A and Y336A took place. Many mutations tended to decrease the methoxychlor-dependent NCoR interaction (L212A, H213A, and Y336A) or totally abolish it (N175A, S251L, T350A, and T350M), while the F171A and I252L mutations elevated the response to methoxychlor by approximately 2- and 3-fold, respectively. In the case of methoxychlor, the data from the M1H and Y2H assays are quite concordant except for the mutations Y336A and T350M (see Table 1). Although the SRC1 and NCoR interactions induced by methoxychlor are slightly decreased with the mutant Y336A, still a small activation by methoxychlor is seen in the M1H assay. On the other hand, the methoxychlor-dependent NCoR interaction is abolished by T350M, but the expected increase in M1H activity is not observed.

For methoxychlor, the two most frequently occurring poses obtained in the docking study are shown in Figure 4a. In one binding mode (shown in yellow in Figure 4a), the trichloride group of methoxychlor is accommodated within a hydrophobic pocket formed by F171, M236, A239, and L249. In this binding mode, very good aromatic interactions are likely to be formed between the phenyl rings of methoxychlor and the residues F227, Y234, and F244. Furthermore, hydrophobic interactions between methoxychlor and F142, I174, F248, and I252 are seen. In the other binding mode (shown in brown in Figure 4a), the trichloride group of methoxychlor is within a hydrophobic cup formed by F142, F171, I174, M178, L216, F227, C229, and Y234. Additional hydrophobic interactions may be formed between methoxychlor and A239, F244, L249, and I252. Interestingly, on the basis of the suitable distance of ~3.0 Å, there could be a hydrogen bond between the methoxy oxygen atom of methoxychlor and the NH_2 group of N175.

From the docking studies, a single preferred docking mode for methoxychlor thus has not been identified, which suggests that the methodology used is unable to pinpoint the likely binding mode (very likely) or that more than one mode of

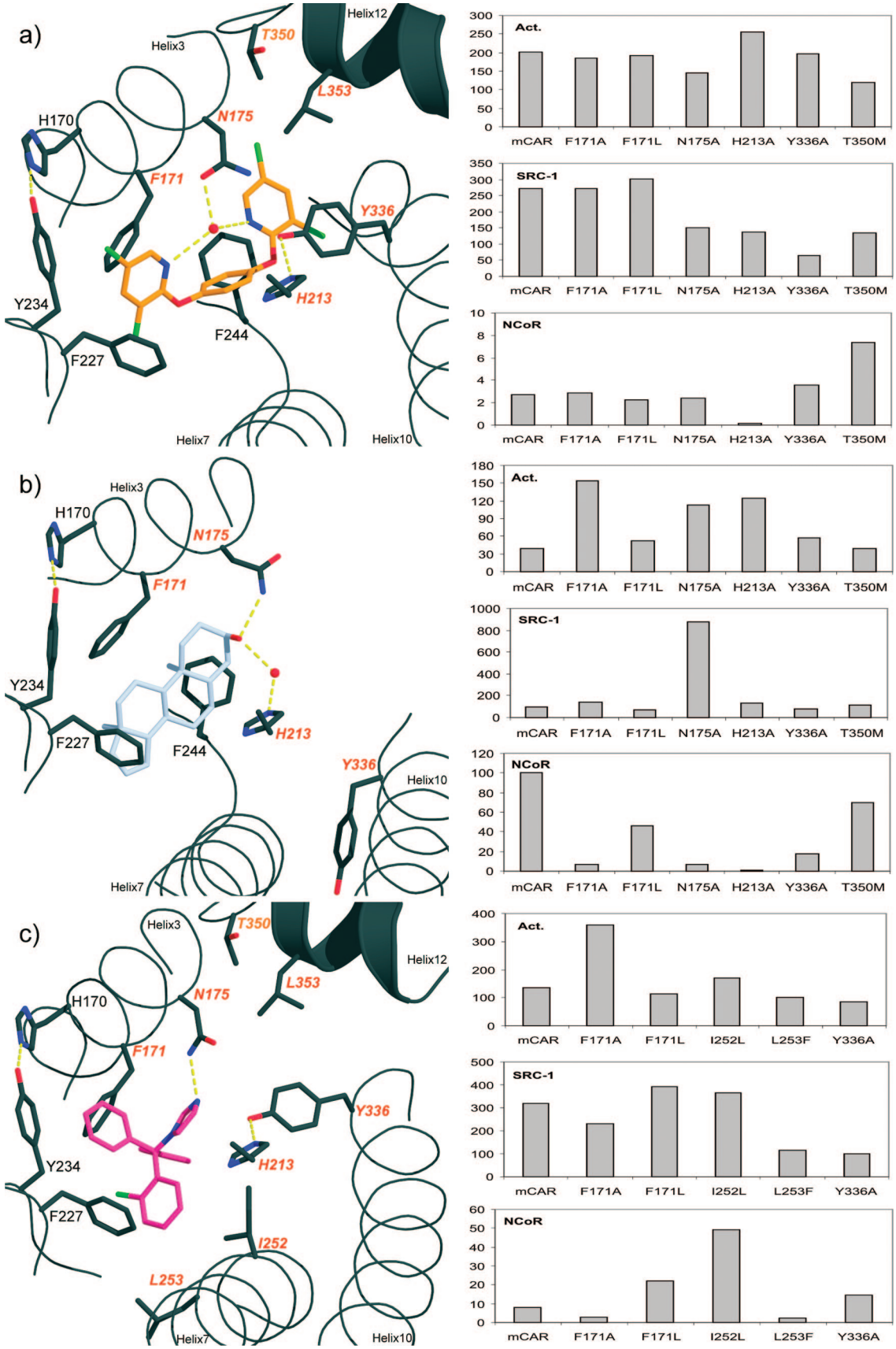

Figure 3. In the left panel, the crystal structures of (a) TCPOBOP[19] and (b) androstenol[18] in complex with mCAR are shown. Here, the secondary structures of helixes H3, H7, H10, and H12 are shown for reference and some of the residues contributing to ligand binding are shown in stick representations and labeled (orange color indicates mutated residues). Possible hydrogen bonds are depicted as yellow dashed lines and conserved water molecules as red spheres. In (c), the possible binding mode of clotrimazole suggested by docking studies is shown. On the right side of the figure, the experimental data for the respective ligand with wild-type mCAR and selected mutants are shown: (top panel) Act = M1H activity; (middle panel) SRC-1 = Y2H assay with coactivator SRC-1; (bottom panel) NCoR = Y2H assay with corepressor NCoR. See Supporting Information Figures S1 and S2 and Materials and Methods for all data and calculations, respectively.

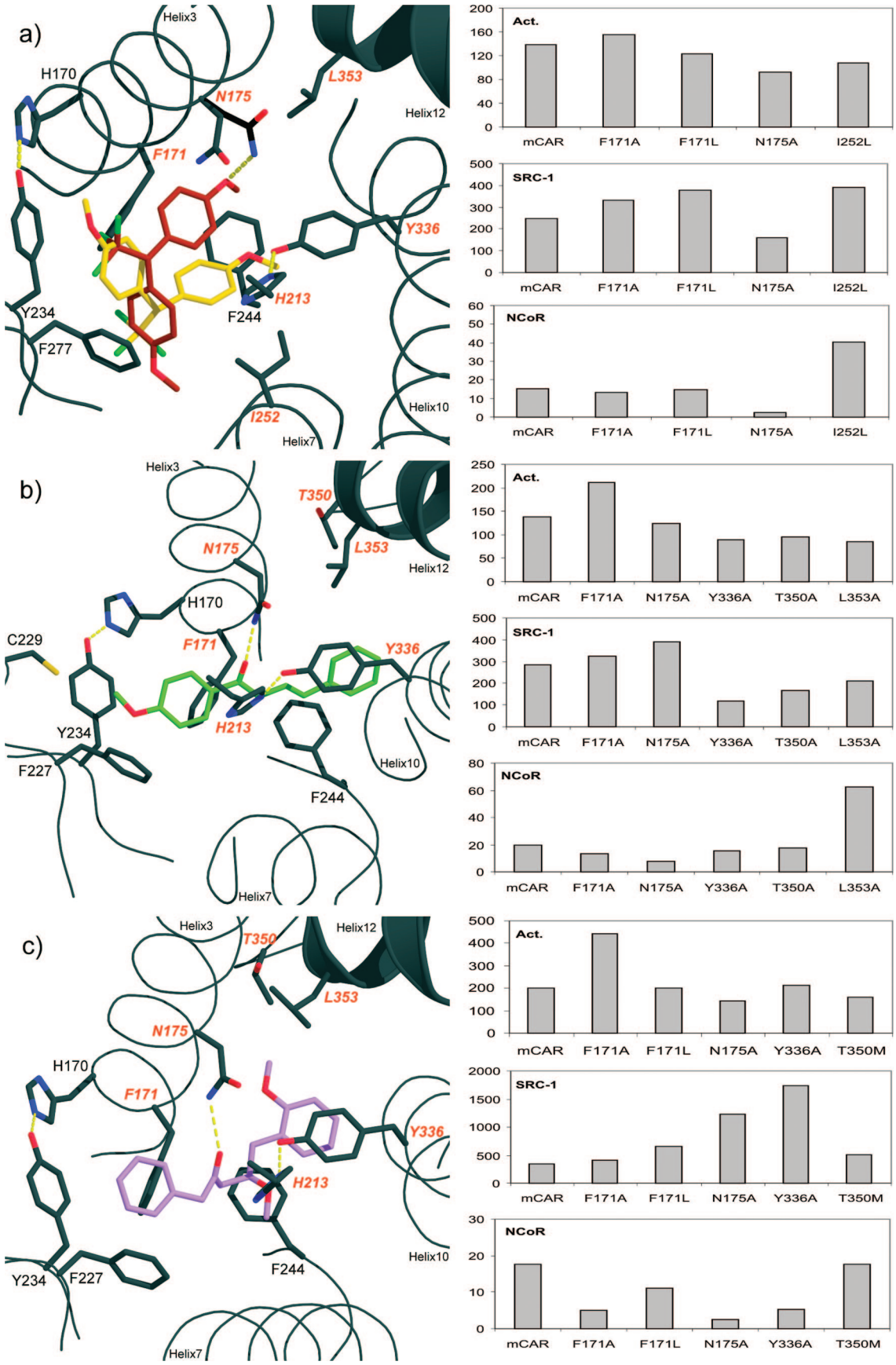

Figure 4. In the left panel, the possible binding modes suggested by the docking studies of (a) methoxychlor, (b) **1**, and (c) **2** to mCAR are shown. For methoxychlor in (a), two docked poses (yellow and brown) were identified (see text for details). The docking results and the experimental data are presented as described in Figure 3.

binding may exist (a rare event). For example, consider the crystal structure of the pregnane X receptor bound to a cholesterol-lowering drug (SR12813):[30] three possible binding modes for the drug were identified; later, a crystal structure in

complex with a coactivator peptide identified only one binding mode that was distinct from the three predicted modes.[31]

Compound 1. Similar to methoxychlor, many mutations had a modulating effect on the response to **1**: the activation by **1** (1.4-fold) was completely abolished with the mutants S251L, Y336A, and T350A and decreased by H213A, I252L, and T350M. The mutation F171A caused a slight increase to 2.1-fold activation by **1**. The −fold magnitude of the SRC-1 interaction was increased by the mutations N175A and I252L, whereas S251L, Y336A, and T350A decreased it by 45−60%. Highly elevated levels of NCoR recruitment in response to **1** were seen with the mutants F171A, F171L, H213A, I252L, and L353A. There were four mutants, where changes in the M1H activation profile could not be explained by data from the Y2H assays (Table 1); for example, despite the observed increase in NCoR interaction by the F171 mutants, an increase in the M1H activation profile was observed.

In most of the docked poses of **1**, the B-ring of **1** is nicely accommodated within a hydrophobic pocket formed by residues F142, F171, I174, M178, L216, F227, C229, and Y234 (the binding mode for **1** that appears most compatible with the binding pocket is shown in Figure 4b). In that pose, the slightly polar methoxy group of the ligand is close to the SH group of C229, where an electrostatic interaction could form. The carbonyl group of **1** is positioned within hydrogen bonding distance (∼2.9 Å) of the NH_2 group of N175. Interestingly, the carbonyl group of **1** is accommodated at the same location as the conserved water in the TCPOBOP-bound structure of mCAR.[19] At the other end of the pocket, the A-ring of **1** is surrounded by the following hydrophobic residues: L216, F244, F248, L249, Y336, L340, L346, and L353, leading to excellent orientation of the ring stacking interactions between the A-ring of **1** and F244, F248, and Y336.

Compound 2. The activation elicited by **2** (2.0-fold) was clearly reduced to 1.3- to 1.4-fold by the N175A, H213A, and T350A mutants, while it was increased to 4.4-fold by F171A. The **2**-induced interaction with SCR-1 was highly elevated (>150%) by the mutations N175A, L212A, and Y336A and even moderately (>50%) by F171L, I252L, and T350M. An increase in NCoR recruitment by **2** was seen with the mutation I252L only. Regardless of the observed increase in coactivator interaction by N175A and T350M or a decrease in the NCoR interaction by L253F, a reduction in the M1H activation profile of **2** was observed with these mutations (Table 1).

The majority of obtained docked poses for **2** are positioned so that the B-ring is sandwiched between F142, F171, F227, and Y234 (see Figure 4c for the binding mode of **2** that appears most compatible with the binding site). The aromatic stacking interactions seem to be very good, and in addition, I174, M178, and L216 would contribute to the hydrophobic environment around the B-ring of **2**. The location of the carbonyl group varies greatly within the docking poses. There is a possibility that the carbonyl group would form hydrogen bonds with either the NH_2 group of N175 or the OH group of Y336, and similar to **1**, the carbonyl group of **2** is located at the same position as the conserved water molecule in the mCAR crystal structure bound to TCPOBOP. At the other end of the molecule, the A-ring appears to form good ring stacking interactions with F244, F248, and Y336 and hydrophobic interactions with L340, L346, and L353. The polar methoxy group attached to the A-ring is surrounded by the polar amino acids N175 and T350.

EE2. EE2 activation was abolished with the mutations N175A, T350A, and T350M, while F171A induced a small increase in EE2 activation. The relative capability of EE2 to recruit SRC-1 was increased by the mutations N175A and L212A, while a >30% decrease took place with the mutations S251L, L253F, and T350A. The already notable recruitment of NCoR by EE2 was significantly increased only by the I252L mutant, whereas significant attenuation (>50%) occurred with all of the tested mutations except for F171A, F171L, and L353A. Although an increase in the recruitment of SRC-1 was observed by N175A, still in the M1H assay, the activation by EE2 was abolished with the same mutant. Another difference between data from the Y2H and M1H assays was observed with the mutant I252L, which significantly increased the EE2-induced NCoR interaction, but only a minor decrease in the M1H-activation profile was observed. Furthermore, regardless of the observed reduction (∼60%) in the EE2-induced NCoR interaction by T350M, the mutation abolished EE2-induced activation in the M1H assay.

The flexible nature of the mCAR binding pocket enables the positioning of EE2 in several different ways within the LBP, even though the molecule contains an acetylene group at C17 that extends perpendicular to the plane of the ring system. In our docking results, we see one of two major conformations for EE2: either (1) the D-ring is buried within the LBP of mCAR and the A-ring is interacting with helix H7 and the β-sheet (Figure 5a) or (2) it is the A-ring that is accommodated deep within the pocket (Figure 5b).

In one binding mode, the 17α-OH group in the D-ring interacts with N175 in helix H3 while the acetylene group is buried in between F171 and F244 (Figure 5a). Alternatively in the poses of this cluster, the acetylene group could interact with F171 and I174 or, induced by a 180° flip around the plane of EE2 ring system, the acetylene group could interact with L212. The distance between the 3-OH group in the A-ring and the main-chain carbonyl group of E225 is ∼2.7 Å, suggestive of a possible hydrogen bond (Figure 5a). In addition, the A-ring interacts with L253 in helix H7. In this binding pose, hydrophobic interactions are formed between the methyl group of EE2 and L212 and L216, while residues F171, I174, F227, Y234, A239, F244, F248, L249, and I252 create the overall hydrophobic environment for the steroid ring structure of EE2.

In the other binding mode, the A-ring is buried deep within the LBP below Y336, where the A-ring is sandwiched between L340 from helix H10, L346 from the linker helix, and L353 from helix H12 (Figure 5b). The D-ring is positioned in the middle of the binding pocket with the acetylene group interacting with L216, while there are no direct hydrogen bonding possibilities for the 17α-OH group apart from the solvent in the LBP.

3. Discussion

It is well-known that the mCAR LBP is promiscuous in terms of recognizing with moderate affinity many ligands of very different molecular structures. There is, however, only one crystal structure of mCAR in complex with an agonist available.[19] In this structure, the superagonist TCPOBOP is well accommodated within the pocket of mCAR, forming specific hydrophobic and hydrogen-bonding interactions with the receptor. Our earlier docking attempts to this structure using the more traditional rigid receptor docking algorithms were not successful in placing the ligand into the LBP or in producing poses with reasonable interactions between the ligand and the receptor (data not shown). This was not a surprise, since earlier studies have pointed out the importance of the initial protein structure in docking studies and the possible bias that is introduced when crystal structures in complex with ligands are used.[32] In the

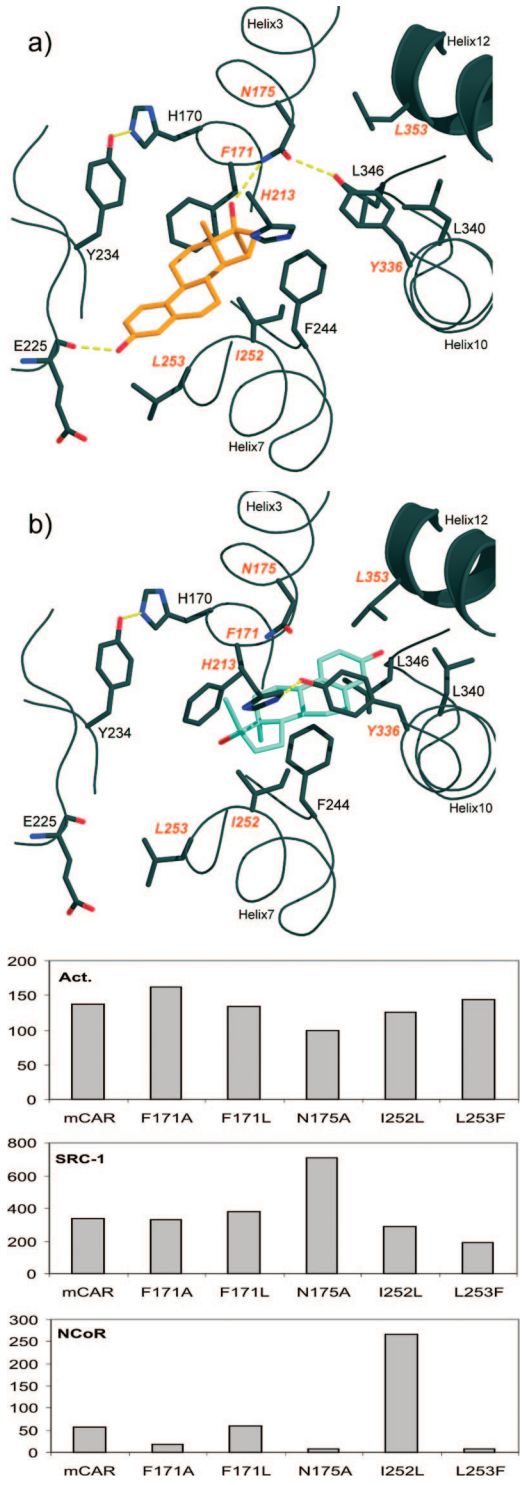

Figure 5. Two possible binding modes for EE2 were suggested by the docking results: orange in (a) and cyan in (b) (see text for details). The docking results and the experimental data are presented as described in Figure 3.

study presented here, we investigated other moderately active, druglike mCAR agonists that might have more relevance for general induction of drug metabolism than TCPOBOP. Thus, in order to introduce some flexibility into the docking process, the Induced Fit Docking protocol of Schrödinger was used in this study.

On the basis of our analysis, it has proved very beneficial to consider multiple docking runs with different settings for the investigated ligands; eight different runs, each run invoking a different set of conditions, were used for each ligand, and multiple docking poses were obtained from each run. Beforehand, it was not possible to determine which protocol would be the most appropriate for each ligand. In general, the differences between the eight runs in terms of the generated ligand poses were minor, but ultimately the most optimal poses in terms of the suggested interactions between protein and ligand atoms of each ligand (manually chosen) were obtained from separate runs.

In this study, we found that it was best to define the LBP for docking attempts by creating a grid based on the centroid of amino acids at the binding site instead of using the centroid of the ligand from the crystal structure, as the latter strategy would probably have resulted in a docking grid biased toward the orientation of TCPOBOP within LBP.

The number of poses obtained from an IFD run depends on the cutoff values used. In this study, the runs that applied the Standard Precision (SP) scoring function generally produced fewer poses compared with the runs that employed the Extra Precision (XP) scoring function. The default cutoff values, however, were used in all of the docking runs, and thus, the docking protocols differed only in the type of the scoring function that was used. The XP scoring function has been designed to take into account hydrophobic enclosure effects,[33] which, on the basis of the known crystal structures of mCAR and our docking studies, is one of the key features in ligand recognition by mCAR. This provides a possible explanation of why the XP scoring function produced more and better poses in this study.

Mutations Affecting the Ligand-Independent Interactions of mCAR. According to our experiments, two mutations, L353A and H213A, abolished both the basal and the ligand-induced interactions between SRC-1 and mCAR. In order to understand the mechanisms by which these mutations affect the function of the receptor, we analyzed the crystal structure of mCAR in complex with TCPOBOP[19] (see Figure 2 for the location of the mutated residues within the LBP of mCAR). L353 is located within helix H12, where it forms a key hydrophobic interaction between the helix H12 and the rest of the protein, thus helping to position the H12 helix in the active conformation, which is crucial for the formation of the AF-2 recognition surface. In the majority of NRs, there is a bulky hydrophobic residue (Leu, Ile, Met, or Phe) at the corresponding position, and mutations of this residue dramatically impair the coactivator interaction and/or the ligand binding ability of several NRs.[25,34−37] The same principle applies for mCAR, where the L353A mutation may disrupt the interaction between helix H12 and the rest of the LBD, thus leading to impaired coactivator binding.

H213 is located within helix H5, which belongs to the middle layer of the three-layered NR sandwich structure. The side chain of H213 points away from the surface and into the LBP of mCAR, where it forms electrostatic interactions with H256 and Y336. In order to compensate for the space created by the H213A mutation, helix H5 would very likely need to move toward the LBP. This would require that helix H3 move closer to the LBP, too. Because helices H3 and H10 participate in the formation of the coactivator binding surface,[19] even the slightest movement of either of the helices would affect coactivator binding. In contrast to L353A, the H213A mutation did not result in a complete loss of activity because we still could detect activation by TCPOBOP but only in the trans-activation assay. It seems plausible that cellular coactivators other than SRC-1 may bind to the mutated receptor (H213A) and that only the

helix H12 mutation (L353A) impairs the binding of all coactivators.

The largest increase in the basal interaction of mCAR with NCoR was observed with the mutation L212A. In order to investigate the possible role of L212 in NCoR recruitment, we studied the crystal structure of the inverse agonist (androstenol) bound to mCAR.[18] This structure, however, lacks a corepressor peptide, and therefore, we superimposed the complex of human PPARα and the SMRT corepressor peptide[38] with the mCAR crystal structure. While L212 might not contact the corepressor directly, it is located directly "beneath" the corepressor binding surface. The space created by the L212A mutation is most likely compensated by a small movement of helix H3, which would allow the corepressor to form better contacts with the ligand-free receptor. Interestingly, the L212A mutation decreases both the basal interaction of SRC-1 with mCAR and the trans-activation potential by about 75−80%, supporting the theory that L212A would create a binding surface preferring corepressors over coactivators. Differential effects on corepressor versus coactivator binding were also seen for the thyroid hormone receptor when a single surface residue was mutated.[39] Another possibility is that L212A disrupts the conformation of the linker helix and AF-2 by inducing a similar collapse of the helix H10 structure as androstenol does.[18] However, the change in NCoR interaction induced by L212A is quite small (6-fold) compared to recruitment induced by androstenol (50-fold), and therefore, the first option might be more likely.

Mutations Affecting the Ligand Recognition of mCAR. We observed an approximately 50% decrease in basal SRC-1 recruitment, a significant decrease in NCoR recruitment by androstenol, and dramatic decrease in basal trans-activation by the mutation F171A. A partial explanation for the decrease in the basal activity is lower expression of the F171A mutant (Supporting Information Figure S3). However, such a decrease in expression was not seen with the human receptor F161A (Jyrkkärinne et al.[25] and unpublished results). Others have reported that the F171A mutation decreases the basal activity of full-length mCAR by 40% and attenuated the androstenol-mediated repression[18] and that the F171W mutation decreased the basal association of coactivator TIF2 by approximately 50%.[19] Altogether, these findings indicate a key role for F171 in the basal activity and androstenol recognition by mCAR. In the crystal structures of mCAR, F171 occupies a very central position in the LBP, forming interactions with the ligands TCPOBOP and androstenol.

In this study, we investigated the role of F171 in ligand binding in more detail and analyzed the effects of F171L and F171A on the binding of six agonists and the inverse agonist androstenol. Our results suggest that aromaticity and the size of the residue at sequence position 171 are not important for the binding of TCPOBOP. In addition, the mutations at residue 171 had only a very small effect on the ligand-induced activation of mCAR by methoxychlor and EE2. The SRC-1 interaction induced by **1** and **2** was increased with F171L to 30% and 85%, respectively. In our docking studies, **1** and **2** are docked so that the B-ring of the molecules forms an aromatic interaction with F171; however, this is not the only aromatic interaction that the B-ring forms with mCAR; the residues F142, F227, and Y234 are also involved. As a result of these aromatic interactions, perhaps aromaticity of the residue 171 is not the key factor for **1** and **2** induced activation. This is further supported by the M1H assay, where F171A significantly increased the activity induced by **1** and **2**. Interestingly, different from the F171A mutation, F171L did not eliminate the inhibition by androstenol but only slightly decreased it.

In contrast to the other ligands, the nature of the residue at position F171 seems to be very important for clotrimazole-induced coregulator interaction. In the M1H assay, clotrimazole is the only agonist that shows a dramatically different response to mutation at position 171 (activation was decreased by F171L but increased by F171A). These results are in part supported by the Y2H assays, where clotrimazole-induced SRC-1 interaction was slightly reduced by F171A while F171L increased slightly the SRC-1 interaction and significantly the NCoR interaction (Figure 3c). It seems that the F171L mutation together with bound clotrimazole stabilizes the coregulator binding surface so that both corepressors and coactivators may bind, which leads to a competitive situation between the two coregulators. The net effect would be the reduced activity of clotrimazole in the M1H assay. According to our docking studies, clotrimazole does not fit perfectly into the mCAR pocket regardless of the induced fit effect used in our docking studies. Only the F171A mutation (but not F171L) seems to create enough space to position clotrimazole so that a stable coactivator binding surface can be formed. This view is supported by the IFD run where clotrimazole was docked into the structure of mCAR where F171 was replaced by an alanine residue: in comparison with clotrimazole docked to the wild-type structure, clotrimazole moved by about 1.2 Å toward A171 and thus overlapped the same space as the side chain of F171 in the wild-type structure.

The residue T350 has previously been implicated in the recognition of TCPOBOP but not of androstenol,[19,23] findings that were reproduced here. We also noted that mutation of T350 into methionine (the corresponding residue in hCAR) but not to alanine resulted in an increase of clotrimazole-elicited activation and SRC-1 recruitment. In the docked complex of clotrimazole and mCAR, there are no direct interactions with T350; indeed, because of the shape of the ligand, there is unoccupied space between clotrimazole and residues F244, Y336, L340, and T350 of mCAR. Methionine has an extended, flexible nonpolar side chain. Hence, when it replaces T350, it may be able to occupy the space between clotrimazole and mCAR and lead to improved interactions moderating any local collapse of the structure.

Species Differences Affecting the Basal and Ligand-Dependent Interaction of CAR. Asparagine at position 175 is one of the very few polar residues in the LBP of mCAR. The mutation N175A does not affect the basal activity of mCAR, but it did induce a clear reduction in the basal interaction between SRC-1 and mCAR, while the weak NCoR interaction remains intact. The basal activity of hCAR, in contrast, is clearly decreased by N165A, and a dramatic increase in basal NCoR interaction is observed.[25] The increase in the NCoR interaction with hCAR by N165A explains the reduced activity, while in mouse our experimental results suggest that coactivators other than SRC-1 contribute to the basal activity. On the other hand, on the basis of our experimental results, N175 is one of the key residues for mediating ligand-induced activity and also androstenol-mediated inhibition of mCAR, while in hCAR, N165A did not consistently affect the ligand-dependent activation or inhibition.[25] However, fewer ligands were tested in that study.

In mCAR, the androstenol-elicited inhibition and recruitment of NCoR are abolished by N175A. In human, however, the same mutation N165A enhances the androstenol-induced NCoR interaction.[25] In the crystal structure of mCAR bound to

androstenol (PDB code 1XNX[18]), the 3α-hydroxyl group of the A-ring of androstenol is coordinated by two hydrogen bonds: to the NH_2 group of N175 and to a water molecule, which is also coordinated by a hydrogen bond to the Nϵ atom of H213 (Figure 3b). In order to investigate the effect of the mutation, we computationally "mutated" N175 to alanine in the available crystal structures of mCAR bound to TCPOBOP and to androstenol and docked androstenol into the mutated structures (see Supporting Information Figure S4). The docking results suggest that with the N175A mutation androstenol might bind conversely compared to what is observed for androstenol bound in the crystal structure of the wild-type mCAR; the D-ring of androstenol would be buried in the LBP and the 3α-hydroxyl group of the A-ring would interact with L253 in helix H7, similar to one of the binding modes the docking study suggested for EE2. But the nonplanar A-ring together with the 3α-hydroxyl group of androstenol would not be able to form a hydrogen bond with the main chain of E225, as suggested for EE2. In addition, if N175 is mutated to alanine, Y336 will most likely reorient itself back to the LBP to form a hydrogen bond with H213 (instead of the water molecule observed in the crystal structure), which could be the reason for the experimentally observed androstenol-induced SRC-1 interaction by N175A. Altogether, our experimental and docking results suggest that in contrast to hCAR, N175 is a key residue for the androstenol-mediated coregulator interactions in mCAR.

Tyrosine 336 occupies a central position in the LBP of CAR, and the importance of Y336 for the basal activity of both mCAR and hCAR is evident from previous mutagenesis studies.[19,20,25] The available crystal structures of human and mouse CAR[19,40] in complex with agonists show that Y336 forms key interactions with the ligands. In addition, molecular dynamics simulations of ligand-free hCAR have suggested that a hydrogen bond between Y326 and N165 stabilizes Y326 into a position where it mimics a bound ligand, thus enabling the active conformation of helix H12.[25,41] In line with these observations, our results show a 90% reduction in the basal activity of mCAR by the mutation Y336A and a reduction of about 80% in the basal interaction between mCAR and SRC-1, while the weak NCoR interaction remained intact. There are, however, interesting differences in the ligand-induced SRC-1 interaction with mCAR. With Y336A, the agonists TCPOBOP, clotrimazole, methoxychlor, and **1** show a clear decrease in the ligand-induced SRC-1 interaction, while the extent of the SRC-1 interaction elicited by **2** is increased. On the basis of the suggested binding mode of **2** (Figure 4c), the A-ring of **2** could occupy the location of the Y336 side chain in the alanine mutant and then form stabilizing hydrophobic interactions with the linker helix. In addition, the methoxy group attached to the A-ring could form electrostatic interactions with N175, which would additionally stabilize the coactivator binding surface. The structures of **1** and **2** are crucially different in this respect because in the A-ring of **1** there is no methoxy group capable of forming interactions with the side chain of a polar residue like N175.

We have previously identified that the major differences within the LBP between hCAR and mCAR are located in helix H7 (S251, I252, and L253 in mCAR) and that F243 in hCAR (L253 in mCAR) determines the species difference in response to EE2.[25] In order to investigate the role of this region in ligand binding to mCAR, we individually mutated these residues to their human counterparts. Very interestingly, in our assays, we saw a dramatic increase in the ligand-induced NCoR interaction with all ligands (except for TCPOBOP) by I252L. In regard to ligand-specific effects, the mutation S251L eliminated the activation induced by **1** while L253F eliminated the clotrimazole-dependent activation. In our docked complexes of clotrimazole with mCAR one of the rings of clotrimazole is surrounded by F227, I252, and L253. It is possible that the change in size and shape of phenylalanine in the L253F mutation could be sufficient to prevent the positioning of clotrimazole within the LBP; as already noted, space to accommodate clotrimazole appears to be limited in the wild-type structure, and L253F would exacerbate the situation.

Whereas the F243L mutant in hCAR led to activation by EE2,[25] in mCAR the introduction of the human residue at that position in the L253F mutant did not alter the wild-type agonist effect of EE2. In mCAR, the L253F mutant decreased the EE2-induced SRC-1 interaction to ∼60% and eliminated the NCoR interaction, but it did not significantly affect the EE2-induced activation in the transactivation assays, which suggests that in mCAR, factors other than merely the type of residue at position 253 regulate the response to EE2. This is also supported by the preferences for different coregulators by human and mouse CAR bound to EE2. Upon binding to wild-type hCAR, EE2 clearly acts as an inverse agonist and does not recruit SRC-1;[25] while being an agonist for the wild-type mCAR, EE2 recruits both SRC-1 and NCoR to a significant extent.[24]

In our docking studies, we show two binding modes for EE2, one of which positions the A-ring of EE2 in contact with L253. If docked in this way (Figure 5a), the 17α-OH group in the D-ring of EE2 could form a hydrogen bond with the side chain of N175 and the 3-OH group of the A-ring could hydrogen-bond with the main-chain carbonyl of E225 at the opposite end of the pocket. This binding mode would appear to stabilize interactions that support the positioning of helix H12 into the active conformation, and this binding mode could also rationalize the observed SRC-1 recruitment by EE2[24] and also some of the effects of mutations (e.g., activation by EE2 of the hCAR mutant F243L).[25] In contrast, androstenol is smaller, lacks a second polar group, and only poorly occupies the LBP.[18] Jyrkkärinne et al.[25] have suggested that EE2 would interfere with helix H12 in hCAR, which would account for the inverse agonism of EE2. The alternative binding mode of EE2 to mCAR shown in Figure 5b, if true, would be consistent with that view and explain the ability of EE2 to also recruit NCoR.[24] These binding modes are quite plausible, but whether either of these two binding modes is relevant to mCAR or hCAR will require further study.

4. Conclusions

We have identified key residues for ligand binding in mCAR and tested the effects of mutations in functional assays. Our results provide novel information about the role of these residues both in ligand binding and on the basal activity of mCAR. We have used an induced-fit protocol for ligand docking in order to generate and evaluate hypotheses regarding the relationship between the experimental results and the location of the bound ligands in the LBP. Our interpretations are admittedly complicated by the fact that changes to any particular residue might affect not only ligand binding but local packing of secondary structure elements and more globally the conformation of the LBD, which is intimately involved in the recognition of coactivators and corepressors. We show that some mutations can positively or negatively modulate the basal activity but the response in the presence of ligand is not necessary the same. Furthermore, our studies clearly demonstrate the species differences in the function of CAR and emphasize the need to understand in detail how mCAR and hCAR interact with their

ligands. This information could be important in the drug development process, where the investigated drug compounds are initially tested for safety in rodents. As a result of the species differences in ligand recognition by CAR, and its role in metabolism and elimination of xenobiotics, the biological responses observed in mouse for a specific compound could be dramatically different in human.

5. Materials and Methods

Chemicals. Androstenol was bought from Steraloids Inc. (Newport, RI). The synthesis of TCPOBOP,[42] **1**,[43] and **2**[27] have been described. Deoxyoligonucleotides were bought from Sigma-Genosys (Cambridge, U.K.). Clotrimazole, methoxychlor, EE2, and other compounds were from Sigma Chemical Co. (St. Louis, MO).

Plasmids. The UASx4-tk-luc reporter and CMX-GAL4 expression plasmids were kind gifts from Dr. R. M. Evans (Salk Institute, La Jolla, CA). The control plasmid pCMVβ was purchased from BD Clontech (Palo Alto, CA). The mouse CAR LBD (residues 118−358) was cloned into CMX-GAL4 as described.[44] Various point mutations introduced into the mCAR LBD (based either on alanine replacements or on sequence differences between mouse and human CAR) were introduced with the QuikChange mutagenesis kit (Stratagene, La Jolla, CA), and the plasmids were purified with ion-exchange columns and verified by restriction mapping and dideoxy sequencing. These mCAR fusion proteins are thought to spontaneously migrate to the nucleus in continuous cell lines because the strong nuclear localization signal (NLS) is present in helix H10 (residues 313−319) of mCAR.[45] The NLS is not affected by the present mutations, and the GAL4 domain also contains an additional NLS.[46]

The yeast two-hybrid system (BD Clontech) plasmid pGBKT7 was used to express the wild-type and point-mutated mCAR LBD, and the pGADT7 plasmid harbored either the NR interaction domain from mouse the coactivator SRC-1 or the mouse corepressor NCoR.[23,44]

Mammalian mCAR Trans-Activation (M1H) Assays. Transient transfection assays with wild-type and mutant mCAR constructs, UASx4-tk-luc reporter, and pCMVβ were done in HEK293 cells essentially as previously described.[23,44] Cells were cultured in the presence of dimethyl sulfoxide (DMSO, 0.1% v/v) or final concentrations of test chemicals (TCPOBOP 1 μM; clotrimazole 2 μM; methoxychlor, **1**, **2**, EE2, and androstenol 10 μM). These concentrations were deemed saturating (EC_{50} of TCPOBOP, 0.05 μM; EC_{50} of androstenol, 0.2 μM) or above the apparent EC_{50} but low enough to exclude any toxicity (EC_{50} values of clotrimazole, **1**, **2**, EE2, ~3 μM; EC_{50} of methoxychlor, >5 μM). The mCAR EC_{50} values are available from the literature for TCPOBOP, androstenol, and methoxychlor,[26,47] and they are well in line with our results. Twenty-four hours after transfection, cells were lysed and luciferase and β-galactosidase activities were determined using the Victor2 multiplate reader (PerkinElmer Wallac, Turku, Finland). All luciferase activities were normalized to the level of β-galactosidase expression and are reported as mean values ± standard deviation from three independent experiments. The reference activity was that determined with the empty GAL4 expression vector (GAL4 only = 1.0).

We have optimized this assay carefully with respect to cell line, culture conditions, and transfection times and have measured CAR activation for more than 200 different chemicals (e.g., see refs 23, 44, and 48). The performance parameter (Z') for this optimized assay was 0.76, and coefficients of variation were typically below 15%, which indicate an excellent and a reproducible assay.[49]

The cells transfected with mCAR constructs were analyzed by Western blotting using the anti-GAL4 antibody. The data indicated that no major differences in the expression levels between the wild-type or mutant mCAR receptors were seen apart from a 50% decrease with the mutant F171A (Supporting Information Figure S3).

Yeast Two-Hybrid (Y2H) Assays. Yeast colonies that expressed wild-type or mutant mCAR LBD plus the interacting partner (NCoR or SRC-1) were selected on SD plates lacking both leucine and tryptophan. Randomly picked colonies were pooled and amplified, and aliquots of yeast cells were treated with DMSO or test chemicals for 3.5 h before measurement of β-galactosidase activities and cell densities as described in detail elsewhere.[24,44] The normalized β-galactosidase activities are expressed as mean values ± standard deviation from two independent determinations, each with triplicate samples. We chose the SRC-1 reference activity as wild-type mCAR + SRC1, treated with DMSO (=100), in analogy with mammalian mCAR activity measurements. This activity corresponds roughly to 30 mU, which is about 15−20% in strength of the well-established p53-T antigen interaction,[50] and it can be further activated by 3- to 4-fold by typical mCAR ligands. In contrast, the basal interaction in the absence of added ligands between mCAR and NCoR was very low, and thus, a more stable activity [10 μM androstenol (=100)] must be selected for reference as before.[24] The yeast strains carrying only one plasmid (mCAR LBD, SRC1, or NCoR) gave activities almost indistinguishable from the background, below 5% level of the mCAR−SRC1 interaction,[24] and they could not be reliably used as references against which to express ligand-dependent changes between experiments.

Docking Studies. Ligand molecules were built and energy-minimized using LigPrep (version 2.0, Schrödinger, LLC, New York, 2005) with the default settings and the OPLS_2005 force field. The crystal structure of mCAR in complex with the agonist TCPOBOP (PDB code 1XLS)[19] was obtained from the PDB[51] and prepared and energy-minimized with the default settings of the Protein Preparation Wizard in the Schrödinger package (Protein Preparation Wizard, Schrödinger Suite 2007, New York, 2005). All water molecules present in the crystal structure were deleted prior to the docking runs.

Docking studies were performed using the Induced Fit Docking (IFD) protocol of Schrödinger (IFD; Schrödinger Suite 2007 Induced Fit Docking Protocol; Glide, version 4.05, Schrödinger, LLC, New York, 2005; Prime, version 1.6, Schrödinger, LLC, New York, 2005). The process of docking using this protocol is explained in detail elsewhere,[52] but in brief, the steps are the following: (1) Initial Glide docking is made to the rigid protein structure using a softened van der Waals potential in order to be able to accommodate for more steric clashes in the initial poses; (2) refinement was done using Prime, including local side chain optimization and energy minimization of protein−ligand complexes from the previous step; (3) ligands are then docked a second time with Glide into the low-energy induced-fit structures from step 2; (4) the binding energy (IFDScore) of each ligand conformation is estimated.

The IFD protocol of Schrödinger is a rather new approach, and hence, the number of published docking studies using the approach is very limited.[52,53] As noted by Sherman et al., 2006, a reasonable initial docking pose for the ligand is crucial for the success of the IFD study. In order to work toward this goal, we explored whether the way the binding pocket was defined affected the outcome of the docking and we particularly investigated whether more space in the binding site created by the replacement of side chains with alanine in the initial Glide docking step of IFD would improve the obtained docking results. We also separately implemented the standard precision (SP) and the extra precision (XP) scoring functions of Glide[33,54] in order to ascertain the optimal scoring function in the case of mCAR.

Altogether, eight IFD runs with different settings were performed for each ligand (Table 3). The binding pocket was defined either as the centroid of the ligand (TCPOBOP) bound within the crystal structure of mCAR or as the centroid of two different sets of four residues from the binding site that were manually chosen. In the IFD protocol, it is possible to temporarily replace flexible residues with alanine in order to assist with the softened-potential docking in step 1, above. Sherman et al.[52] present four rules for the selection of residues to be replaced by alanine, and on the basis of these rules, we identified for replacement two residues, L346 and L353, with missing electron density and high *B*-factors in the mCAR

Table 3. Induced-Fit Docking Runs and Used Settings

run no.	scoring function	centroid of[a]	replaced residues[b]
1	SP	ligand	
2	SP	ligand	Y336, L346, L353
3	SP	ligand	N175, L346, L353
4	XP	ligand	
5	XP	ligand	Y336, L346, L353
6	XP	ligand	N175, L346, L353
7	XP	F142, F171, H213, F248	
8	XP	H213, C229, F248, L346	

[a] The binding site was defined either as a centroid of the ligand present in the crystal structure of the target protein or as a centroid of a set of binding site residues. [b] In the soft docking step of the induced-fit docking protocol additional space was created within the binding site by replacing flexible residues with alanine.

crystal structure. In addition, N175 and Y336 had high *B*-factors and were also chosen for replacement by alanine. Because of the very hydrophobic nature of the mCAR binding pocket, in all of the docking runs, the hydrogen bond energy cutoff filter of Glide was set to 0 kcal/mol in step 1. For the rest of the docking procedure, the default settings of the IFD protocol were used.

Clustering of Docking Results. The docked conformations for each ligand from eight separate runs were analyzed with a program that defines a descriptor for each conformation (freely available from http://web.abo.fi/fak/mnf/bkf/research/johnson/software.php). First, and for every docking pose, each ligand atom−protein atom pair was listed. If the distance between the atoms was less than the cutoff, then "1" was appended to a descriptor vector, but if the distance was larger than the cutoff, then "0" is appended. For all ligands, a cutoff value of 3.0 Å was used, except for clotrimazole, for which a cutoff of 2.7 Å was applied in order to increase the discrimination among similar binding poses. For a single ligand, all observed conformations were compared with each other as the number of shared atom contacts among each pair of conformations. The resulting similarity matrix was then used as input to the Markov cluster algorithm,[55] in which the default settings were used except for the inflation option, which was set to 3.0 for clotrimazole, methoxychlor, and **2**; for all other ligands the default value of 2.0 was used. This option affects the granularity of the obtained clusters, meaning that an increase in the inflation value leads to an increase in the number of obtained clusters while a decrease in the value leads to a reduced number of clusters.

Visualization. The Bodil modeling environment was used for visualization of the model and the template structures as well as for the visualization of the docking results.[56] Figures were produced with PyMOL, version 1.1.[57]

Acknowledgment. We thank Heidi Kidron for her comments on the manuscript, Raita Sallinen and Lea Pirskanen for help with the assays, and Mikko Huhtala, Santeri Puranen, and Robin Sundström for technical assistance. This work was supported by TEKES National Agency for Technology, Academy of Finland, the Sigrid Jusélius Foundation, National Graduate School in Informational and Structural Biology, Foundation of Åbo Akademi University (Center of Excellence Program in Cell Stress) and Tor, Joe, and Pentti Borg's Memorial Fund.

Supporting Information Available: Data from mammalian trans-activation, yeast two-hybrid and Western blotting assays, and a detailed description of the induced-fit docking results. This material is available free of charge via the Internet at http://pubs.acs.org.

References

(1) Chawla, A.; Repa, J. J.; Evans, R. M.; Mangelsdorf, D. J. Nuclear receptors and lipid physiology: opening the X-files. *Science* **2001**, *294*, 1866–1870.

(2) Maglich, J. M.; Sluder, A.; Guan, X.; Shi, Y.; McKee, D. D.; Carrick, K.; Kamdar, K.; Willson, T. M.; Moore, J. T. Comparison of complete nuclear receptor sets from the human, *Caenorhabditis elegans* and *Drosophila genomes*. *Genome Biol* **2001**, *2*, RESEARCH0029.

(3) Francis, G. A.; Fayard, E.; Picard, F.; Auwerx, J. Nuclear receptors and the control of metabolism. *Annu. Rev. Physiol.* **2003**, *65*, 261–311.

(4) Moras, D.; Gronemeyer, H. The nuclear receptor ligand-binding domain: structure and function. *Curr. Opin. Cell Biol.* **1998**, *10*, 384–391.

(5) Li, Y.; Lambert, M. H.; Xu, H. E. Activation of nuclear receptors: a perspective from structural genomics. *Structure* **2003**, *11*, 741–746.

(6) Rosenfeld, M. G.; Glass, C. K. Coregulator codes of transcriptional regulation by nuclear receptors. *J. Biol. Chem.* **2001**, *276*, 36865–36868.

(7) Aranda, A.; Pascual, A. Nuclear hormone receptors and gene expression. *Physiol Rev* **2001**, *81*, 1269–1304.

(8) Hu, X.; Lazar, M. A. Transcriptional repression by nuclear hormone receptors. *Trends Endocrinol. Metab.* **2000**, *11*, 6–10.

(9) Honkakoski, P.; Sueyoshi, T.; Negishi, M. Drug-activated nuclear receptors CAR and PXR. *Ann. Med.* **2003**, *35*, 172–182.

(10) Handschin, C.; Meyer, U. A. Induction of drug metabolism: the role of nuclear receptors. *Pharmacol. Rev.* **2003**, *55*, 649–673.

(11) Timsit, Y. E.; Negishi, M. CAR and PXR: the xenobiotic-sensing receptors. *Steroids* **2007**, *72*, 231–246.

(12) Choi, H. S.; Chung, M.; Tzameli, I.; Simha, D.; Lee, Y. K.; Seol, W.; Moore, D. D. Differential transactivation by two isoforms of the orphan nuclear hormone receptor CAR. *J. Biol. Chem.* **1997**, *272*, 23565–23571.

(13) Dussault, I.; Lin, M.; Hollister, K.; Fan, M.; Termini, J.; Sherman, M. A.; Forman, B. M. A structural model of the constitutive androstane receptor defines novel interactions that mediate ligand-independent activity. *Mol. Cell. Biol.* **2002**, *22*, 5270–5280.

(14) Forman, B. M.; Tzameli, I.; Choi, H. S.; Chen, J.; Simha, D.; Seol, W.; Evans, R. M.; Moore, D. D. Androstane metabolites bind to and deactivate the nuclear receptor CAR-beta. *Nature* **1998**, *395*, 612–615.

(15) Sueyoshi, T.; Kawamoto, T.; Zelko, I.; Honkakoski, P.; Negishi, M. The repressed nuclear receptor CAR responds to phenobarbital in activating the human CYP2B6 gene. *J. Biol. Chem.* **1999**, *274*, 6043–6046.

(16) Tzameli, I.; Pissios, P.; Schuetz, E. G.; Moore, D. D. The xenobiotic compound 1,4-bis[2-(3,5-dichloropyridyloxy)]benzene is an agonist ligand for the nuclear receptor CAR. *Mol. Cell. Biol.* **2000**, *20*, 2951–2958.

(17) Huang, W.; Zhang, J.; Wei, P.; Schrader, W. T.; Moore, D. D. Meclizine is an agonist ligand for mouse constitutive androstane receptor (CAR) and an inverse agonist for human CAR. *Mol. Endocrinol.* **2004**, *18*, 2402–2408.

(18) Shan, L.; Vincent, J.; Brunzelle, J. S.; Dussault, I.; Lin, M.; Ianculescu, I.; Sherman, M. A.; Forman, B. M.; Fernandez, E. J. Structure of the murine constitutive androstane receptor complexed to androstenol: a molecular basis for inverse agonism. *Mol. Cell* **2004**, *16*, 907–917.

(19) Suino, K.; Peng, L.; Reynolds, R.; Li, Y.; Cha, J.-Y.; Repa, J. J.; Kliewer, S. A.; Xu, H. E. The nuclear xenobiotic receptor CAR: structural determinants of constitutive activation and heterodimerization. *Mol. Cell* **2004**, *16*, 893–905.

(20) Andersin, T.; Väisänen, S.; Carlberg, C. The critical role of carboxy-terminal amino acids in ligand-dependent and -independent transactivation of the constitutive androstane receptor. *Mol. Endocrinol.* **2003**, *17*, 234–246.

(21) Windshügel, B.; Jyrkkärinne, J.; Vanamo, J.; Poso, A.; Honkakoski, P.; Sippl, W. Comparison of homology models and X-ray structures of the nuclear receptor CAR: assessing the structural basis of constitutive activity. *J. Mol. Graphics Modell.* **2007**, *25*, 644–657.

(22) Poso, A.; Honkakoski, P. Ligand recognition by drug-activated nuclear receptors PXR and CAR: structural, site-directed mutagenesis and molecular modeling studies. *Mini-Rev. Med. Chem.* **2006**, *6*, 937–947.

(23) Jyrkkärinne, J.; Mäkinen, J.; Gynther, J.; Savolainen, H.; Poso, A.; Honkakoski, P. Molecular determinants of steroid inhibition for the mouse constitutive androstane receptor. *J. Med. Chem.* **2003**, *46*, 4687–4695.

(24) Mäkinen, J.; Reinisalo, M.; Niemi, K.; Jyrkkärinne, J.; Chung, H.; Pelkonen, O.; Honkakoski, P. Dual action of oestrogens on the mouse constitutive androstane receptor. *Biochem. J.* **2003**, *376*, 465–472.

(25) Jyrkkärinne, J.; Windshügel, B.; Mäkinnen, J.; Ylisirniö, M.; Peräkylä, M.; Poso, A.; Sippl, W.; Honkakoski, P. Amino acids important for ligand specificity of the human constitutive androstane receptor. *J. Biol. Chem.* **2005**, *280*, 5960–5971.

(26) Stanley, L. A.; Horsburgh, B. C.; Ross, J.; Scheer, N.; Wolf, C. R. PXR and CAR: nuclear receptors which play a pivotal role in drug disposition and chemical toxicity. *Drug Metab Rev* **2006**, *38*, 515–597.

(27) Pulkkinen, J.; Vepsäläinen, J. 3-Unsubstituted 1,5-diaryl-2,4-pentanediones and -4-methoxypentanones: synthesis via corresponding 3-hydroxy ketones generated from 2-isoxazolines. *J. Org. Chem.* **1996**, *61*, 8604–8609.
(28) Pulkkinen, J.; Honkakoski, P.; Peräkylä, M.; Berczi, I.; Laatikainen, R. Synthesis and evaluation of estrogen agonism of diaryl 4,5-dihydroisoxazoles, 3-hydroxyketones, 3-methoxyketones, and 1,3-diketones: a compound set forming a 4D molecular library. *J. Med. Chem.* **2008**, *51*, 3562–3571.
(29) Ozers, M. S.; Ervin, K. M.; Steffen, C. L.; Fronczak, J. A.; Lebakken, C. S.; Carnahan, K. A.; Lowery, R. G.; Burke, T. J. Analysis of ligand-dependent recruitment of coactivator peptides to estrogen receptor using fluorescence polarization. *Mol. Endocrinol.* **2005**, *19*, 25–34.
(30) Watkins, R. E.; Wisely, G. B.; Moore, L. B.; Collins, J. L.; Lambert, M. H.; Williams, S. P.; Willson, T. M.; Kliewer, S. A.; Redinbo, M. R. The human nuclear xenobiotic receptor PXR: structural determinants of directed promiscuity. *Science* **2001**, *292*, 2329–2333.
(31) Watkins, R. E.; Davis-Searles, P. R.; Lambert, M. H.; Redinbo, M. R. Coactivator binding promotes the specific interaction between ligand and the pregnane X receptor. *J. Mol. Biol.* **2003**, *331*, 815–828.
(32) Murray, C. W.; Baxter, C. A.; Frenkel, A. D. The sensitivity of the results of molecular docking to induced fit effects: application to thrombin, thermolysin and neuraminidase. *J. Comput.-Aided Mol. Des.* **1999**, *13*, 547–562.
(33) Friesner, R. A.; Murphy, R. B.; Repasky, M. P.; Frye, L. L.; Greenwood, J. R.; Halgren, T. A.; Sanschagrin, P. C.; Mainz, D. T. Extra precision glide: docking and scoring incorporating a model of hydrophobic enclosure for protein−ligand complexes. *J. Med. Chem.* **2006**, *49*, 6177–6196.
(34) Chen, S.; Johnson, B. A.; Li, Y.; Aster, S.; McKeever, B.; Mosley, R.; Moller, D. E.; Zhou, G. Both coactivator LXXLL motif-dependent and -independent interactions are required for peroxisome proliferator-activated receptor gamma (PPARgamma) function. *J. Biol. Chem.* **2000**, *275*, 3733–3736.
(35) Stehlin, C.; Wurtz, J. M.; Steinmetz, A.; Greiner, E.; Schäle, R.; Moras, D.; Renaud, J. P. X-ray structure of the orphan nuclear receptor RORbeta ligand-binding domain in the active conformation. *EMBO J.* **2001**, *20*, 5822–5831.
(36) Kumar, M. B.; Fujimoto, T.; Potter, D. W.; Deng, Q.; Palli, S. R. A single point mutation in ecdysone receptor leads to increased ligand specificity: implications for gene switch applications. *Proc. Natl. Acad. Sci. U.S.A.* **2002**, *99*, 14710–14715.
(37) Wang, M.; Thomas, J.; Burris, T. P.; Schkeryantz, J.; Michael, L. F. Molecular determinants of LXRalpha agonism. *J. Mol. Graphics Modell.* **2003**, *22*, 173–181.
(38) Xu, H. E.; Stanley, T. B.; Montana, V. G.; Lambert, M. H.; Shearer, B. G.; Cobb, J. E.; McKee, D. D.; Galardi, C. M.; Plunket, K. D.; Nolte, R. T.; Parks, D. J.; Moore, J. T.; Kliewer, S. A.; Willson, T. M.; Stimmel, J. B. Structural basis for antagonist-mediated recruitment of nuclear co-repressors by PPARalpha. *Nature* **2002**, *415*, 813–817.
(39) Marimuthu, A.; Feng, W.; Tagami, T.; Nguyen, H.; Jameson, J. L.; Fletterick, R. J.; Baxter, J. D.; West, B. L. TR surfaces and conformations required to bind nuclear receptor corepressor. *Mol. Endocrinol.* **2002**, *16*, 271–286.
(40) Xu, R. X.; Lambert, M. H.; Wisely, B. B.; Warren, E. N.; Weinert, E. E.; Waitt, G. M.; Williams, J. D.; Collins, J. L.; Moore, L. B.; Willson, T. M.; Moore, J. T. A structural basis for constitutive activity in the human CAR/RXRalpha heterodimer. *Mol. Cell* **2004**, *16*, 919–928.
(41) Windshügel, B.; Jyrkkärinne, J.; Poso, A.; Honkakoski, P.; Sippl, W. Molecular dynamics simulations of the human CAR ligand-binding domain: deciphering the molecular basis for constitutive activity. *J. Mol. Model.* **2005**, *11*, 69–79.
(42) Honkakoski, P.; Moore, R.; Gynther, J.; Negishi, M. Characterization of phenobarbital-inducible mouse Cyp2b10 gene transcription in primary hepatocytes. *J. Biol. Chem.* **1996**, *271*, 9746–9753.
(43) Burton, H.; Munday, D. Acylation and allied reactions catalyzed by strong acids. XVI. Reactions of some omega-phenylalkanoyl perchlorates. *J. Chem. Soc.* **1957**, 1718–1726.
(44) Mäkinen, J.; Frank, C.; Jyrkkärinne, J.; Gynther, J.; Carlberg, C.; Honkakoski, P. Modulation of mouse and human phenobarbital-responsive enhancer module by nuclear receptors. *Mol. Pharmacol.* **2002**, *62*, 366–378.
(45) Zelko, I.; Sueyoshi, T.; Kawamoto, T.; Moore, R.; Negishi, M. The peptide near the C terminus regulates receptor CAR nuclear translocation induced by xenochemicals in mouse liver. *Mol. Cell. Biol.* **2001**, *21*, 2838–2846.
(46) Chan, C. K.; Jans, D. A. Synergy of importin alpha recognition and DNA binding by the yeast transcriptional activator GAL4. *FEBS Lett.* **1999**, *462*, 221–224.
(47) Blizard, D.; Sueyoshi, T.; Negishi, M.; Dehal, S. S.; Kupfer, D. Mechanism of induction of cytochrome p450 enzymes by the proestrogenic endocrine disruptor pesticide-methoxychlor: interactions of methoxychlor metabolites with the constitutive androstane receptor system. *Drug Metab. Dispos.* **2001**, *29*, 781–785.
(48) Honkakoski, P.; Palvimo, J. J.; Penttilä, L.; Vepsäläinen, J.; Auriola, S. Effects of triaryl phosphates on mouse and human nuclear receptors. *Biochem. Pharmacol.* **2004**, *67*, 97–106.
(49) Iversen, P. W.; Eastwood, B. J.; Sittampalam, G. S.; Cox, K. L. A comparison of assay performance measures in screening assays: signal window, Z′ factor, and assay variability ratio. *J. Biomol. Screening* **2006**, *11*, 247–252.
(50) Mäkinen, J.; Peterson, S.; Honkakoski, P. Teaching the basics of nuclear receptor action: a simple laboratory exercise using the yeast two-hybrid method. *Am. J. Pharm. Educ.* **2005**, *69*, 176−183 (Article 26).
(51) Berman, H. M.; Westbrook, J.; Feng, Z.; Gilliland, G.; Bhat, T. N.; Weissig, H.; Shindyalov, I. N.; Bourne, P. E. The Protein Data Bank. *Nucleic Acids Res.* **2000**, *28*, 235–242.
(52) Sherman, W.; Day, T.; Jacobson, M. P.; Friesner, R. A.; Farid, R. Novel procedure for modeling ligand/receptor induced fit effects. *J. Med. Chem.* **2006**, *49*, 534–553.
(53) Gadakar, P. K.; Phukan, S.; Dattatreya, P.; Balaji, V. N. Pose prediction accuracy in docking studies and enrichment of actives in the active site of GSK-3beta. *J. Chem. Inf. Model.* **2007**, *47*, 1446–1459.
(54) Friesner, R. A.; Banks, J. L.; Murphy, R. B.; Halgren, T. A.; Klicic, J. J.; Mainz, D. T.; Repasky, M. P.; Knoll, E. H.; Shelley, M.; Perry, J. K.; Shaw, D. E.; Francis, P.; Shenkin, P. S. Glide: a new approach for rapid, accurate docking and scoring. 1. Method and assessment of docking accuracy. *J. Med. Chem.* **2004**, *47*, 1739–1749.
(55) Van Dongen, S. Ph.D. Thesis, University of Utrecht, The Netherlands, 2000.
(56) Lehtonen, J.; Still, D.-J.; Rantanen, V.-V.; Ekholm, J.; Björklund, D.; Iftikhar, Z.; Huhtala, M.; Repo, S.; Jussila, A.; Jaakkola, J.; Pentikäinen, O. T.; Nyrönen, T.; Salminen, T.; Gyllenberg, M.; Johnson, M. S. BODIL: a molecular modeling environment for structure−function analysis and drug design. *J. Comput.-Aided Mol. Des.* **2004**, *18*, 401–419.
(57) DeLano, W. L. *The PyMOL Molecular Graphics System*; DeLano Scientific LLC: Palo Alto, CA, 2007; http://www.pymol.org.

JM800337R